Macular Atrophy Development and Subretinal Drusenoid Deposits in Anti-Vascular Endothelial Growth Factor Treated Age-Related Macular Degeneration

Anna V. Zarubina,[1] Orly Gal-Or,[2,3] Carrie E. Huisingh,[1] Cynthia Owsley,[1] and K. Bailey Freund[2,4]

[1]Department of Ophthalmology, School of Medicine; University of Alabama at Birmingham, Birmingham, Alabama, United States
[2]Vitreous Retina Macula Consultants of New York, New York, New York, United States
[3]Rabin Medical Center, Petach-Tikva, Israel
[4]Department of Ophthalmology, New York University School of Medicine, New York, New York, United States

Correspondence: K. Bailey Freund, Vitreous Retina Macula Consultants of New York, 460 Park Avenue, New York, NY 10022, USA; kbfnyf@aol.com.

Submitted: June 7, 2017
Accepted: October 29, 2017

Citation: Zarubina AV, Gal-Or O, Huisingh CE, Owsley C, Freund KB. Macular atrophy development and subretinal drusenoid deposits in anti-vascular endothelial growth factor treated age-related macular degeneration. *Invest Ophthalmol Vis Sci.* 2017;58:6038–6045. DOI:10.1167/iovs.17-22378

Purpose. To explore the association between presence of subretinal drusenoid deposits (SDD) at baseline in eyes with neovascular age-related macular degeneration (nAMD) with the development of macular atrophy (MA) during anti-vascular endothelial growth factor (VEGF) therapy.

Methods. There were 74 eyes without pre-existing MA receiving anti-VEGF therapy for nAMD for 2 years or longer analyzed. At least two image modalities that included spectral-domain optical coherence tomography, near-infrared reflectance, fluorescein angiography, and color fundus photos were used to assess for SDD presence, phenotype (dot and ribbon), and location, neovascularization type, and MA. Logistic regression models using generalized estimating equations assessed the association between SDD and the development of MA adjusting for age, neovascularization type, and choroidal thickness.

Results. SDD were present in 46 eyes (63%) at baseline. MA developed in 38 eyes (51%) during the mean of 4.7 ± 1.2 years of follow-up. Compared with eyes without SDD, those with SDD at baseline were 3.0 times (95% confidence interval [CI] 1.1–8.5, $P = 0.0343$) more likely to develop MA. Eyes with SDD present in the inferior macula and inferior extramacular fields at baseline were 3.0 times and 6.5 times more likely to develop MA at follow-up than eyes without SDD in these locations (95% CI 1.0–8.9, $P = 0.0461$ and 95% CI 1.3–32.4, $P = 0.0218$, respectively). MA development was not associated with a specific SDD phenotype.

Conclusions. MA frequently developed in eyes during anti-VEGF treatment. SDD were independently associated with MA development. The extension of SDD into the inferior fundus, particularly in the inferior extramacular field, conferred higher odds of subsequent MA development.

Keywords: anti-VEGF, geographic atrophy, neovascular age-related macular degeneration, reticular pseudodrusen, subretinal drusenoid deposits

Macular atrophy (MA) is a common occurrence during treatment of neovascular age-related macular degeneration (nAMD) with intravitreal anti-vascular endothelial growth factor (VEGF) therapy.[1–3] Like typical geographic atrophy (GA) occurring in non-nAMD, MA associated with anti-VEGF therapy for nAMD is characterized by the loss of the outer retina, retinal pigment epithelium (RPE), and choriocapillaris (CC).[2,4–6] Some authors have noted that, compared with typical GA, MA occurring in the setting of anti-VEGF therapy is often smaller in size but with a more diffuse distribution.[6] Zanzottera et al.[7,8] showed histologic differences in RPE morphology, basal laminar deposit (BLamD), and the descent of the external limiting membrane toward Bruch's membrane at the atrophy border in eyes with non-neovascular versus those with nAMD.

The occurrence of macular atrophy in treated eyes is a common cause of poor long-term visual function following initial short-term visual gains.[1,9,10] Development of prevention and treatment strategies for MA will be enabled through a better understanding of its pathophysiology and risk factors. Decreased central choroidal thickness,[11,12] presence of type 3 neovascularization (NV),[1,13,14] and pre-existing MA[1] in the fellow eye are known to herald the appearance of MA during anti-VEGF treatment. Atrophic macular changes have been noted in the eyes of mice with genetically downregulated RPE-derived VEGF[15] and the deleterious effect of anti-VEGF drugs on VEGF production by RPE has been suspected in humans.[1,16]

Subretinal drusenoid deposits (SDD), often referred to by their reticular pattern seen on en face images as reticular pseudodrusen, have been linked to MA.[11,16,17] SDD are extracellular conglomerates of unesterified cholesterol and various types of proteins located between RPE and photoreceptors[18] that are visualized on optical coherence tomography (OCT) and en face imaging modalities in two morphologically distinctive forms, "dots" and "ribbons."[19] SDD have been described in the settings of outer retinal ischemia and loss of photoreceptors, RPE, and choriocapillaris.[20–22] The cause and effect of these lesions are yet to be ascertained. While some researchers consider SDD to be a marker of outer retinal ischemia resulting from choroidal hypoxia due to local[21] or systemic vascular factors,[23] others propose that SDD them-

Copyright 2017 The Authors

This work is licensed under a Creative Commons Attribution-NonCommercial-NoDerivatives 4.0 International License.

Downloaded from iovs.arvojournals.org on 12/02/2020

selves are able to disrupt metabolic pathways needed for photoreceptor and RPE survival resulting in their loss and subsequent CC atrophy.[20] Despite the similarities in conditions under which MA and SDD are observed, relationships between these two entities remain poorly understood.

The goal of this study is to explore the relationship between SDD morphology and localization and MA development in patients undergoing intravitreal anti-VEGF therapy for nAMD.

Methods

This study design was approved by Western institutional review board (Olympia, WA, USA). It complied with the Health Insurance Portability and Accountability Act of 1996 and followed the tenets of the Declaration of Helsinki.

Participants

Data collection and imaging analysis were described in detail previously.[14] In brief, data from 82 consecutive patients (88 eyes) were retrospectively collected. Among those, 71 patients (74 eyes) met the inclusion criteria below. All patients were followed by a single physician (KBF) at two offices of the Vitreous Retina Macula Consultants of New York (New York, NY, USA).

Inclusion criteria for this study were as follows: (1) 50 years and older, (2) any untreated NV lesion type in one or both eyes at baseline, (3) administration of any anti-VEGF agent (ranibizumab, bevacizumab, aflibercept) on a continuous treat-and-extend regimen (TER) for at least 2 years before this review, and (4) availability of eye-tracked spectral-domain (SD) OCT B-scans, near-infrared reflectance (NIR), color digital fundus photographs (CFP), and fluorescein angiography (FA) at baseline and SD-OCT B-scans and NIR at the last follow-up visit.

Exclusion criteria were as follows: (1) any previous treatment for NV (photodynamic therapy, intravitreal steroids or anti-VEGF, thermal laser), (2) presence of GA, MA secondary to NV, subfoveal fibrosis, RPE tears, and NV secondary to maculopathies other than AMD at baseline, and (3) the spherical equivalent exceeding the range of ± 2 diopters (D).

Basic demographics (age, sex, and race), as well as information about smoking status (ever or never smoker), and comorbidities (cardiovascular disease, hypertension, diabetes, hypercholesterolemia/hyperlipidemia) were collected as part of routine self-reported medical history at baseline.

Imaging Modalities

Eye-tracked SD-OCT images were obtained with the Spectralis HRA + OCT (Heidelberg Engineering, Inc., Franklin, MA, USA). Macula volumes were centered over the fovea with at least 19 horizontal B-scans across an area of 20° × 15°. NIR ($\lambda = 830$ nm) images with 30° field of view centered over the macula were acquired with the confocal scanning laser ophthalmoscope (Spectralis HRA + OCT). These images were analyzed with the AutoRescan function of the Spectralis software that allowed spatial point-to-point correlation between SD-OCT and NIR. CFP with 50° view centered over the macula were taken with the Topcon TRC ×501 fundus camera (Topcon Imagenet, Tokyo, Japan). FA images were obtained with either the confocal scanning laser ophthalmoscope (Spectralis HRA + OCT) or the Topcon TRC ×501 fundus camera. All images were acquired after pupil dilation.

Image Processing and Grading

The grading of NV lesion types, MA detection, and the measurement of subfoveal choroidal thickness (SCT) were assessed at baseline and described in detail previously.[14] In brief, the anatomic classification of NV was defined as type 1 (sub-RPE), type 2 (subretinal), or type 3 (intraretinal/retinal angiomatous proliferation) based on grading of SD-OCT and FA images at baseline.[14,24] When multiple NV types were present in one eye, the lesion was classified as "mixed" type, but with each constituent type specified. MA was considered present when: (1) on NIR there was a hyperreflective area with a sharp border spanning at least 250 μm in the maximum linear dimension and not adjacent to peripapillary chorioretinal atrophy, and (2) on SD-OCT this area corresponded to the degeneration of RPE and outer retina with hypertransmission into the choroid.[14,25] MA grading was performed at both baseline and follow-up visits. Using calipers available in the SD-OCT review software, SCT was measured under the fovea at a single location between the outer border of RPE/Bruch's membrane complex and the choroidal-scleral junction on the foveal SD-OCT B-scan at both baseline and follow-up visits.[12] The type of NV and MA area were assessed by two independent graders blinded to patients' data followed by an open adjudication with a senior grader (KBF) in cases of disagreement.

Separate analyses were performed for three categories of SDD: SDD of any phenotype, ribbon phenotype SDD, and dot phenotype SDD. The grading of SDD and their phenotypes were assessed using SD-OCT, NIR, and CFP based on the multimodal approach described previously.[26,27] In brief, lesions were required to be confirmed by SD-OCT and at least one en face modality or shown by two en face modalities, when lesions were outside the SD-OCT volume. The characteristics of SDD and their two phenotypes were assessed with previously described definitions.[19,26] Briefly, dots form sharp peaks or domes of hyperreflective material in the subretinal space seen on SD-OCT that correspond to discrete yellowish-gray and hyporeflective dots on CFP and NIR, respectively. Ribbons form broad or rounded hyperreflective elevations in subretinal space seen on SD-OCT that correspond to interlocking yellowish-gray and faint hyporeflective ribbons on CFP and NIR, respectively. Five or more lesions of a particular phenotype detected within one of the prespecified locations described below were required for such a phenotype to be considered present in this location.[19] For SDD of any phenotype category, ≥5 lesions of any phenotype had to be present in one such location.[27,28] For the purposes of this study, we identified locations based on the retinal anatomy: macula or extramacular region.[29] The macula was defined as a 6000-μm diameter circle centered at the fovea as determined by the central horizontal SD-OCT B-scan. The extramacular region was defined as the area outside of this 6000-μm diameter circle. The macula and extramacular regions were divided into "superior" and "inferior" areas by the foveal horizontal SD-OCT B-scan (Fig. 1). Thus, a total of four retinal locations were assessed for lesions by the graders: superior macula, superior extramacular, inferior macula, and inferior extramacular. SDD were considered to be present at the eye-level when SDD of any phenotype were present within ≥1 of the prespecified locations. SDD of the ribbon or dot phenotype were considered to be present at the eye-level if SDD of the respective phenotype were present within ≥1 of the prespecified locations.

SDD grading was performed at baseline by two independent graders (AVZ) and (OG-O), who were blinded to the MA status at follow-up. The senior grader (KBF) evaluated in cases of disagreement after an open adjudication.

Statistical Analysis

Baseline characteristics were compared between those with and without SDD using generalized estimating equations (GEE) to account for the within-person correlation. Logistic regression models using GEE were used to evaluate the association

Investigative Ophthalmology & Visual Science

Downloaded from iovs.arvojournals.org on 12/02/2020

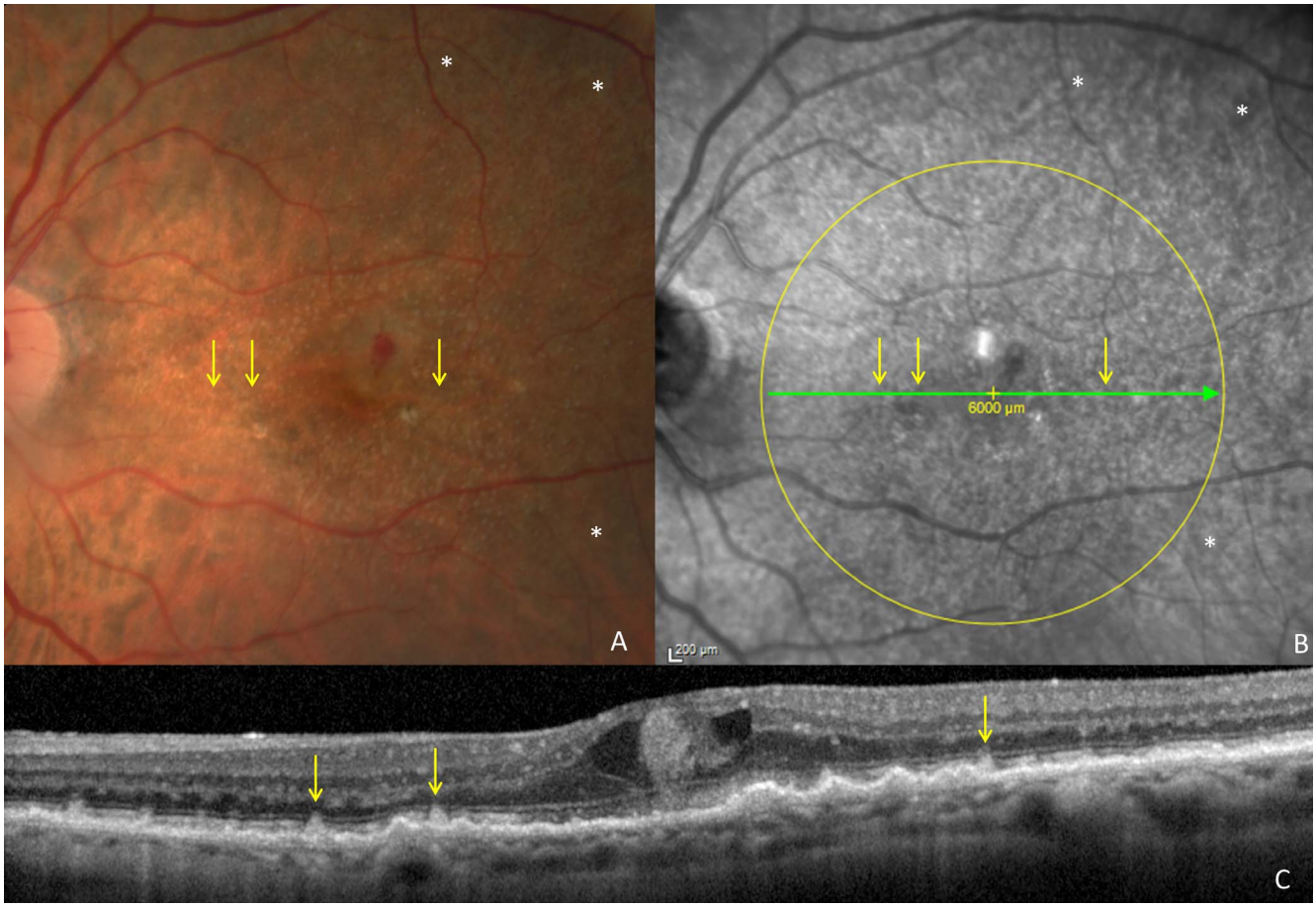

Figure 1. Example of the grading method of SDD in the current study based on the multimodal imaging approach. An eye with type 3 neovascular lesion has visible SDD present in the macula and extramacular fields (**A–C**). The macula is indicated on NIR image by the yellow 6000-µm diameter circle centered on the foveal optical coherent tomography (OCT) B-scan (*green line*) (**B**). Examples of SDD of the dot phenotype demonstrated on the side-by-side CFP (**A**), NIR (**B**), and cross-sectional OCT B-scan (**C**) are indicated by *yellow arrows*. Examples of SDD of the ribbon phenotype demonstrated on the side-by-side CFP (**A**) and NIR (**B**) are indicated by *asterisks*.

between the presence of SDD and the development of MA, and crude and adjusted odds ratios and their 95% confidence intervals (CI) were calculated. Models were adjusted for age alone, then were further adjusted for neovascularization type and choroidal thickness. The odds of MA development was also compared between presence or absence of each SDD phenotype (ribbons and dots) and presence or absence of SDD in each location (superior and inferior macula, superior and inferior extramacula).[30] All statistical analyses were performed using SAS, version 9.3 software (SAS, Cary, NC, USA). $P < 0.05$ were considered statistically significant.

Results

A total of 88 eyes of 82 patients with untreated nAMD at baseline were screened for the current study. Among these eyes, 14 of 88 (16%) had MA at baseline and were excluded from further analysis. The remaining 74 eyes (71 patients) met the inclusion criteria and constituted the study population for the current analysis.

Demographic and clinical characteristics of eyes at baseline are summarized in Table 1. The study group was predominantly white (97%) with female patients comprising 73% of all patients. The mean age of patients was 81 years (range, 52–98 years). Of subjects, 39% were smokers and 23% reported a history of cardiovascular disease. At baseline, most eyes (76%) had type 1 (38%) or type 3 (38%) neovascular lesions, with smaller percentages of type 2 (8%) and mixed (16%) lesions. SDD were present in 63% (46/73 eyes). The mean duration of follow-up was 4.69 ± 1.15 years with a mean of 7.14 ± 2.72 injections per year.

New MA had developed in 51% (38/74) of eyes at the most recent follow-up. Those with SDD at baseline were more likely to develop MA at follow-up compared with those without SDD (63% vs. 30%, $P = 0.0069$). Patients with SDD were more likely to be older ($P = 0.0199$) and have thinner SCT ($P = 0.0009$). Additionally, distribution of NV types varied significantly between eyes with and without SDD ($P = 0.0455$). As prior reports have described an association between thin choroids and MA,[11,12] and between type 3 NV and MA,[1,13] we repeated the analysis using these parameters as binary variables and confirmed their significance ($P = 0.0212$ and $P = 0.0103$, respectively). The lowest SCT quartile was considered pathologic and measured <118 µm, in line with prior reports defining abnormally thin SCT.[31,32] Sex, race, smoking status, and history of hypertension, cardiovascular disease (CVD), diabetes, and hypercholesterolemia/hyperlipidemia were not statistically different by SDD presence. The comparison of clinical characteristics of eyes at baseline with and without SDD is summarized in Table 1.

We further analyzed the relationship between SDD presence and location with MA development, adjusting for the identified confounders (Table 2). Eyes with SDD at baseline

Investigative Ophthalmology & Visual Science

Downloaded from iovs.arvojournals.org on 12/02/2020

Table 1. Demographic and Clinical Characteristics of Patients With nAMD at Baseline; Treatment Characteristics and Macular Atrophy Status at Follow-up in the Overall Study Group and Groups Stratified by SDD Status

		Study Group Stratified by SDD*		
	Overall Study Group (n = 74 Eyes, 100%)	**With SDD (n = 46 Eyes, 63.0%)**	**Without SDD (n = 27 Eyes, 37.0%)**	
	***N* (%) or Mean (±SD)**	***N* (%) or Mean (±SD)**	***N* (%) or Mean (±SD)**	***P* Value**
Age, y	80.71 ± 8.74	82.57 ± 8.48	77.53 ± 8.55	**0.0199**
Female (+)*	54 (72.97)	34 (73.91)	19 (70.37)	0.7473
White (+)	72 (97.30)	45 (97.83)	26 (96.30)	0.7176
CVD (+)†	16 (23.19)	12 (27.27)	4 (16.67)	0.3001
Hypertension(+)‡	43 (63.24)	28 (63.64)	15 (62.50)	0.9259
Diabetes (+)‡	11(16.18)	6 (13.64)	5 (20.83)	0.4633
Hypercholesterolemia/hyperlipidemia (+)‡	13 (19.12)	10 (22.73)	3 (12.50)	0.2395
Smoking (+)§	26 (38.81)	16 (37.21)	9 (39.13)	0.8771
NV type 1 (sub-RPE)	28 (37.84)	13 (28.26)	15 (55.56)	**0.0455**
NV type 2 (subretinal)	6 (8.11)	3 (6.52)	3 (11.11)	
NV type 3 (intraretinal/RAP)	28 (37.84)	22 (47.83)	5 (18.52)	
NV mixed type	12 (16.22)	8 (17.39)	4 (14.81)	
Subfoveal choroidal thickness, μm	163.62 ± 59.08	145.93 ± 54.40	194.19 ± 56.11	**0.0009**
Follow-up, y	4.69 ± 1.15	4.83 ± 1.04	4.41 ± 1.29	0.1633
Number of anti-VEGF injections/y	7.14 ± 2.72	6.90 ± 2.48	7.65 ± 3.06	0.2744
De novo MA at follow-up (+)	38 (51.35)	29 (63.04)	8 (29.63)	**0.0069**

RAP, retinal angiomatous proliferation. Bold font used to denote statistically significant *P* values.
* Missing data for one eye.
† Missing data for five eyes.
‡ Missing data for six eyes.
§ Missing data for seven eyes.

were 3.0 times more likely to develop MA at follow up when compared with eyes without SDD at baseline (odds ratio [OR] 3.0, 95% confidence interval [CI] 1.1–8.5, $P = 0.0343$). Eyes with SDD present in the inferior macula and inferior extramacular field at baseline were 3.0 and 6.5 times more likely to develop MA at follow-up compared with eyes without SDD in these locations at baseline (OR 3.0, 95% CI 1.0–8.9, $P = 0.0461$ and OR 6.5, 95% CI 1.3–32.4, $P = 0.0218$, respectively). The association between SDD presence in the superior macula and the superior extramacular field and MA development was not statistically significant (OR 1.9, 95% CI 0.7–5.3, $P = 0.2193$ and OR 2.1, 95% CI 0.7–6.4, $P = 0.1928$, respectively). Distribution of SDD across the four analyzed fields is shown in Figure 2.

In the overall study group, the presence of SDD with combined ribbon and dot phenotypes was 38% (28/73 eyes). Only 7% (5/73) and 18% (13/73) eyes had isolated ribbon and dot phenotypes, respectively. When analyzing the relationship between SDD phenotype and MA development using the same multivariate regression model (Table 3), the positive association between the presence of SDD of the ribbon phenotype and MA development was not statistically significant (OR 1.6, 95% CI 0.5–4.5, $P = 0.4105$). Similarly, the positive association between SDD of the dot phenotype and

Table 2. Crude and Adjusted Association Between the Presence of SDD and Their Locations at Baseline and MA Development at Follow-up

	Odds of MA Development in the Overall Study Group (n = 73 Eyes)					
	Crude Odds Ratio (95% CI)	***P* Value**	**Adjusted Odds Ratio (95% CI)***	***P* Value**	**Adjusted Odds Ratio (95% CI)†**	***P* Value**
SDD						
Yes	4.1 (1.5–11.2)	**0.0071**	3.4 (1.2–10.0)	**0.0227**	3.0 (1.1–8.5)	**0.0343**
No	Ref.	–	Ref.	–	Ref.	–
SDD in superior macula						
Yes	2.4 (0.9–6.17)	0.0683	2.1 (0.8–5.5)	0.1525	1.9 (0.7–5.3)	0.2193
No	Ref.	–	Ref.	–	Ref.	–
SDD in inferior macula						
Yes	4.0 (1.5–10.6)	**0.0056**	3.6 (1.3–10.0)	**0.0140**	3.0 (1.0–8.9)	**0.0461**
No	Ref.	–	Ref.	–	Ref.	–
SDD in superior extra-macula						
Yes	2.9 (1.1–7.8)	**0.0368**	2.6 (0.9–7.5)	0.0725	2.1 (0.7–6.4)	0.1928
No	Ref.	–	Ref.	–	Ref.	–
SDD in inferior extra-macula						
Yes	6.4 (1.6–25.0)	**0.0075**	6.6 (1.5–30.2)	**0.0145**	6.5 (1.3–32.4)	**0.0218**
No	Ref.	–	Ref.	–	Ref.	–

Bold font used to denote statistically significant *P* values.
* Adjusted for age.
† Adjusted for age, NV type 3, and SCT <118 μm.

Investigative Ophthalmology & Visual Science

Downloaded from iovs.arvojournals.org on 12/02/2020

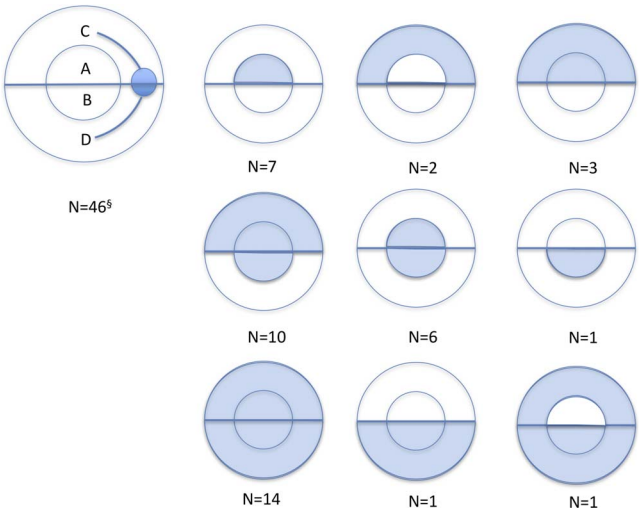

Figure 2. Scheme of SDD distribution across retinal subfields among eyes with SDD at baseline. *Inner circle* represents the macula defined as the 6000-μm diameter area. *Horizontal line* represents the foveal OCT B-scan. *Highlighted areas* represent the retinal subfield where SDD were detected. (**A**) Superior macula; (**B**) inferior macula; (**C**) superior extramacular field; (**D**) inferior extramacular field; *N*, number of eyes. §One eye had SDD limited to peripapillary area only.

MA was also not statistically significant (OR 1.9, 95% CI 0.7–5.3, $P = 0.1946$).

Discussion

We found that while only a minority (16%) of eyes with treatment-naïve nAMD had MA at baseline, 51% of eyes lacking MA at baseline developed MA while receiving anti-VEGF therapy on a TER over a mean follow-up of 4.7 years. This high incidence of MA and its associated loss of visual function is of great concern to clinicians and their patients[6,10,13,33,34] and has generated significant interest in the ophthalmology research community.[15,35–37] We confirm the previously reported association between MA and SDD,[11,16,17] in which the baseline presence of SDD conferred a 3-fold increase of odds of subsequent MA development independent of other factors including age, intraretinal neovascularization, and thin choroid. We ascribe special importance to this association and think that understanding the nature of SDD may shed light on the pathophysiology of MA and explain the link between the two entities. A growing body of histopathologic and observational clinical studies lends support to the RPE origin of SDD. In particular, SDD are thought to result from the derangement of intraretinal lipid metabolism[18] that to a large extent involves RPE cells[38] and have been found to be compositionally similar to and frequently accompany the RPE-derived soft drusen, basal linear deposits, and BLamD[18,39–41]; SDD are dynamic structures[42] and their more advanced stages exhibit slower growth rate[43]; SDD fade out over NV and atrophic areas[44,45] characterized by RPE degeneration.[46]

It seems reasonable to suggest that the RPE is the cellular structure that links SDD and MA development. Several theories have been proposed explaining the relationship between these entities, but with only circumstantial evidence available in their support, all are debatable. According to the proponents of the vascular etiology of MA development, VEGF suppression in the settings of nAMD therapy reduces choriocapillaris permeability with subsequent impaired oxygen and nutrient delivery to the RPE.[1] RPE ischemia may also result from a "steal" phenomenon created by the diversion of blood flow from the choriocapillaris to new pathologic blood vessels[4] or vascular disease recognized by choroidal thinning that was found to be associated with both MA and SDD presence.[11] While no specific mechanism has been proposed to explain these observations, RPE ischemia/hypoxia may lead to upregulation of VEGF production in an attempt to improve endothelial cell permeability and rescue RPE cells by paracrine and autocrine mechanisms, respectively.[35] This, however, may theoretically shift the energy balance away from the phagocytic, lipid, and retinol recycling and other functions of RPE and result in SDD formation in particular. Iatrogenic neutralization of VEGF by anti-VEGF therapy could reduce this rescue mechanism leading to both endothelial and RPE cell loss and subsequent MA. However, in an animal model of RPE ischemia resulting from the sustained systemic VEGF neutralization, direct endothelial toxicity was short-lived and mitigated by increased VEGF production by an otherwise unaffected RPE.[35]

Discovery of complement fragments and other immune system constituents within SDD[39] led some to believe that inflammation plays a part in their formation.[44] Indeed, the single nucleotide polymorphism Y402H of the complement factor H gene results in the increased presence of macrophage attack complexes (MAC) at the interface of Bruch's membrane and choriocapillaris.[47] While MAC are thought to aid in clearance of cellular debris under normal conditions, their increased presence is thought to induce "bystander injury" to the surrounding cells and has been associated with choroid thinning,[47] in which situation SDD may be a byproduct of inflammation generated by complement activation. Also, aging RPE express progressively more immunogenic amyloid precursor protein with subsequent increase in activation of MAC even without high-risk polymorphisms and subsequent sub-RPE drusen formation.[48] In fact, aging itself has been proposed to be the major determinant of RPE cell function relating to the transport of the cholesterol to and from photoreceptors and choriocapillaris.[49] SDD may thus be related to the changes in RPE milieu detrimental to its proper functioning. Intravitreal

Table 3. Crude and Adjusted Association Between SDD Phenotypes at Baseline and MA Development at Follow-up

	Odds of MA Development in the Overall Study Group ($n = 73$ Eyes)					
	Crude Odds Ratio (95% CI)	***P* Value**	**Adjusted Odds Ratio (95% CI)***	***P* Value**	**Adjusted Odds Ratio (95% CI)†**	***P* Value**
Ribbon phenotype						
Yes	2.6 (1.0–6.8)	0.0475	2.2 (0.8–6.1)	0.1232	1.6 (0.5–4.5)	0.4105
No	Ref.	–	Ref.	–	Ref.	–
Dot phenotype						
Yes	2.6 (1.0–6.8)	0.0495	2.2 (0.8–6.0)	0.1311	1.9 (0.7–5.3)	0.1946
No	Ref.	–	Ref.	–	Ref.	–

* Adjusted for age.
† Adjusted for age, NV type 3, and SCT <118 μm.

Downloaded from iovs.arvojournals.org on 12/02/2020

anti-VEGF drugs or *VEGF* gene downregulation may further attenuate the VEGF signal to endothelial cells inducing angiopathic changes[50] that, in turn, could lead to ischemia and tissue loss manifesting as MA. Although almost any permutation of the above theories may explain the pathogenesis of MA and SDD, RPE appears to play the critical role instigating injury to the involved tissues. Further, we propose that SDD with their specific morphology, easily recognizable on different imaging modalities, may serve as a clinical biomarker of RPE dysfunction that may help predict eyes at greater risk for MA.

We found that the presence of SDD in the inferior macula and the inferior extramacular field at baseline conferred a 3.0 and 6.5 increased odds, respectively, of developing MA during the anti-VEGF treatment. Based on the published studies[18,45,51] and our observations, SDD are most frequently present in the upper fundus with subsequent downward advancement into the inferior macula and outward advancement into the superior and inferior extramacular fields. Interestingly, this pattern of SDD distribution is reminiscent of the topography of rods,[52] the age-dependent loss of which is exacerbated by AMD[53] with characteristic cellular and subcellular RPE changes[54] and is possibly linked to RPE dysfunction.[55,56] In contrast, RPE architecture and function in healthy aging eyes remains stable throughout the lifespan.[57] The extent of the SDD spread across the retinal fields is, therefore, likely proportional to the duration and extent of RPE dysfunction and may confer a higher risk of MA development. The significance of SDD pattern of distribution is further supported by the higher risk of late AMD development associated with SDD located outside, but not within the macula.[58]

The association between a specific SDD phenotype and MA development was not statistically significant. This could be explained by the insufficient sample size of our eye cohort and the considerable (~60%) overlap between the dot and ribbon phenotypes, which could conceal a potential effect of SDD phenotype that was of smaller magnitude relative to SDD localization. Notwithstanding, different SDD phenotypes merit recognition, as at least two studies showed that confluent ribbon phenotype was associated with GA development and dot phenotype was associated with nAMD.[30,59]

Similar to some,[16,26,41] but not all[60–62] prior studies, none of the other demographic or clinical characteristics, including female sex, smoking, hypertension, CVD, and diabetes were associated with SDD presence. Our findings, therefore, lend further support to the idea that the pathogenesis of SDD is driven primarily by some local mechanisms and less dependent of systemic factors.

Strength and Limitations

To the best of our knowledge, our systematic categorization of SDD phenotype and location represents the first attempt to relate these parameters to the development of MA. A multimodal approach and standard definitions were rigorously applied by two independent graders to the evaluation of NV lesion types, presence of MA, SDD, and their phenotypes.[19,24,26,27,63–66] The availability of an extended follow-up period allowed us to accurately capture incident MA.[25]

Our work has limitations typical of a retrospective clinic-based study. With the relatively small number of participants and a predominance of females, it is challenging to ascertain sex differences in SDD prevalence within subgroups. The infrequency of isolated ribbon or dot phenotype of SDD could lead to type I error (i.e., failure to detect the significant association of SDD phenotype and MA). Because SD-OCT scans were largely unavailable outside the macula, we were limited to en face imaging modalities for SDD detection, however, other authors employed similar approach to SDD detection outside the SD-OCT volume.[27] Although characterization of spatial relationship between SDD and MA would further inform our understanding of the relationship between these two entities, we could not evaluate SDD adjacency to MA areas at the last follow-up visit because not all patients had CFP required for identifying ribbon SDD[67] which were identified through multimodal imaging.

The growing body of knowledge on SDD established their association with clinically relevant outcomes, such as MA development and early through late AMD incidence and progression.[11,16,17,30,44,58–60,68–70] There is an important need for building consensus on an appropriate SDD classification system that would define the phenotype, distribution, size, and other SDD parameters similar to the way other manifestations of the RPE dysfunction (e.g., soft drusen and pigmentary changes)[71] are defined and currently used in the Age-Related Eye Disease Study classification system. This would allow the future studies to accurately describe the natural history of SDD and their phenotypes, their influence on the evolution early through late AMD, effects of anti-VEGF drugs on SDD development and regression, and their effects on the evolution of nAMD-related MA. Further experimental models targeting specific RPE functions would be valuable in establishing the causative relationship between RPE dysfunction and retinal diseases.

In conclusion, we confirm that MA frequently develops in eyes during anti-VEGF treatment. SDD are independently associated with MA development and potentially share a common pathophysiology stemming from RPE dysfunction. The extension of SDD into the inferior fundus, particularly in the inferior extramacular field, appears to be related to subsequent MA development. Histologic studies and accurate SDD and MA models are needed to further refine the biologic relationship between these two clinically important entities.

Acknowledgments

Supported by grants from the National Institutes of Health (R01AG04212; Bethesda, MD, USA), the Macula Foundation, Inc. (New York, NY, USA), Research to Prevent Blindness (New York, NY, USA), the EyeSight Foundation of Alabama (Birmingham, AL, USA), and the Dorsett Davis Discovery Fund (Birmingham, AL, USA).

Disclosure: **A.V. Zarubina**, None; **O. Gal-Or**, None; **C.E. Huisingh**, None; **C. Owsley**, None; **K.B. Freund**, Optovue (C), Optos (C), Heidelberg Engineering (C), Genentech (C), Graybug Vision (C), Genentech/Roche (F)

References

1. Grunwald JE, Daniel E, Huang J, et al. Risk of geographic atrophy in the comparison of age-related macular degeneration treatments trials. *Ophthalmology*. 2014;121:150–161.
2. Grunwald JE, Pistilli M, Ying GS, et al. Growth of geographic atrophy in the comparison of age-related macular degeneration treatments trials. *Ophthalmology*. 2015;122:809–816.
3. Lois N, McBain V, Abdelkader E, Scott NW, Kumari R. Retinal pigment epithelial atrophy in patients with exudative age-related macular degeneration undergoing anti-vascular endothelial growth factor therapy. *Retina*. 2013;33:13–22.
4. Sarks J, Tang K, Killingsworth M, Arnold J, Sarks S. Development of atrophy of the retinal pigment epithelium around disciform scars. *Br J Ophthalmol*. 2006;90:442–446.
5. Rosenfeld PJ, Shapiro H, Tuomi L, et al. Characteristics of patients losing vision after 2 years of monthly dosing in the phase III ranibizumab clinical trials. *Ophthalmology*. 2011; 118:523–530.

Downloaded from iovs.arvojournals.org on 12/02/2020

6. Schutze C, Wedl M, Baumann B, Pircher M, Hitzenberger CK, Schmidt-Erfurth U. Progression of retinal pigment epithelial atrophy in antiangiogenic therapy of neovascular age-related macular degeneration. *Am J Ophthalmol*. 2015;159:1100–1114.e1.
7. Zanzottera EC, Ach T, Huisingh C, Messinger JD, Spaide RF, Curcio CA. Visualizing retinal pigment epithelium phenotypes in the transition to geographic atrophy in age-related macular degeneration. *Retina*. 2016;36(suppl 1):S12–S25.
8. Zanzottera EC, Ach T, Huisingh C, Messinger JD, Freund KB, Curcio CA. Visualizing retinal pigment epithelium phenotypes in the transition to atrophy in neovascular age-related macular degeneration. *Retina*. 2016;36(suppl 1):S26–S39.
9. Bhisitkul RB, Desai SJ, Boyer DS, Sadda SR, Zhang K. Fellow eye comparisons for 7-year outcomes in ranibizumab-treated AMD subjects from ANCHOR, MARINA, and HORIZON (SEVEN-UP Study). *Ophthalmology*. 2016;123:1269–1277.
10. Rofagha S, Bhisitkul RB, Boyer DS, Sadda SR, Zhang K; for the SEVEN-UP Study Group. Seven-year outcomes in ranibizumab-treated patients in ANCHOR, MARINA, and HORIZON: a multicenter cohort study (SEVEN-UP). *Ophthalmology*. 2013;120:2292–2299.
11. Cho HJ, Yoo SG, Kim HS, et al. Risk factors for geographic atrophy after intravitreal ranibizumab injections for retinal angiomatous proliferation. *Am J Ophthalmol*. 2015;159:285–292.e1.
12. Matsumoto H, Sato T, Morimoto M, et al. Treat-and-extend regimen with aflibercept for retinal angiomatous proliferation. *Retina*. 2016;36:2282–2289.
13. McBain VA, Kumari R, Townend J, Lois N. Geographic atrophy in retinal angiomatous proliferation. *Retina*. 2011;31:1043–1052.
14. Xu L, Mrejen S, Jung JJ, et al. Geographic atrophy in patients receiving anti-vascular endothelial growth factor for neovascular age-related macular degeneration. *Retina*. 2015;35:176–186.
15. Saint-Geniez M, Kurihara T, Sekiyama E, Maldonado AE, D'Amore PA. An essential role for RPE-derived soluble VEGF in the maintenance of the choriocapillaris. *Proc Natl Acad Sci U S A*. 2009;106:18751–18756.
16. Hogg RE, Silva R, Staurenghi G, et al. Clinical characteristics of reticular pseudodrusen in the fellow eye of patients with unilateral neovascular age-related macular degeneration. *Ophthalmology*. 2014;121:1748–1755.
17. Munk MR, Ceklic L, Ebneter A, Huf W, Wolf S, Zinkernagel MS. Macular atrophy in patients with long-term anti-VEGF treatment for neovascular age-related macular degeneration. *Acta Ophthalmol*. 2016;94:e757–e764.
18. Curcio CA, Messinger JD, Sloan KR, McGwin GJ, Medeiros NE, Spaide RF. Subretinal drusenoid deposits in non-neovascular age-related macular degeneration: morphology, prevalence, topography, and biogenesis model. *Retina*. 2013;33:265–276.
19. Suzuki M, Sato T, Spaide RF. Pseudodrusen subtypes as delineated by multimodal imaging of the fundus. *Am J Ophthalmol*. 2014;157:1005–1012.
20. Spaide RF. Outer retinal atrophy after regression of subretinal drusenoid deposits as a newly recognized form of late age-related macular degeneration. *Retina*. 2013;33:1800–1808.
21. Alten F, Clemens CR, Heiduschka P, Eter N. Localized reticular pseudodrusen and their topographic relation to choroidal watershed zones and changes in choroidal volumes. *Invest Ophthalmol Vis Sci*. 2013;54:3250–3257.
22. Xu X, Liu X, Wang X, et al. Retinal pigment epithelium degeneration associated with subretinal drusenoid deposits in age-related macular degeneration. *Am J Ophthalmol*. 2017;175:87–98.
23. Rastogi N, Smith RT. Association of age-related macular degeneration and reticular macular disease with cardiovascular disease. *Surv Ophthalmol*. 2016;61:422–433.
24. Freund KB, Zweifel SA, Engelbert M. Do we need a new classification for choroidal neovascularization in age-related macular degeneration? *Retina*. 2010;30:1333–1349.
25. Abdelfattah NS, Zhang H, Boyer DS, Sadda SR. Progression of macular atrophy in patients with neovascular age-related macular degeneration undergoing antivascular endothelial growth factor therapy. *Retina*. 2016;36:1843–1850.
26. Zarubina AV, Neely DC, Clark ME, et al. Prevalence of subretinal drusenoid deposits in older persons with and without age-related macular degeneration, by multimodal imaging. *Ophthalmology*. 2016;123:1090–1100.
27. De Bats F, Mathis T, Mauget-Faysse M, Joubert F, Denis P, Kodjikian L. Prevalence of reticular pseudodrusen in age-related macular degeneration using multimodal imaging. *Retina*. 2016;36:46–52.
28. Kim JH, Chang YS, Kim JW, Lee TG, Kim CG. Prevalence of subtypes of reticular pseudodrusen in newly diagnosed exudative age-related macular degeneration and polypoidal choroidal vasculopathy in korean patients. *Retina*. 2015;35:2604–2612.
29. Sundaram V, Barsam A, Alwitry A, Khaw P. *Training in Ophthalmology*. 1st ed. New York: Oxford University Press Inc; 2009.
30. Zhou Q, Daniel E, Maguire MG, et al. Pseudodrusen and incidence of late age-related macular degeneration in fellow eyes in the comparison of age-related macular degeneration treatments trials. *Ophthalmology*. 2016;123:1530–1540.
31. Spaide RF. Age-related choroidal atrophy. *Am J Ophthalmol*. 2009;147:801–810.
32. Marsiglia M, Boddu S, Chen CY, et al. Correlation between neovascular lesion type and clinical characteristics of non-neovascular fellow eyes in patients with unilateral, neovascular age-related macular degeneration. *Retina*. 2015;35:966–974.
33. Kumar N, Mrejen S, Fung AT, Marsiglia M, Loh BK, Spaide RF. Retinal pigment epithelial cell loss assessed by fundus autofluorescence imaging in neovascular age-related macular degeneration. *Ophthalmology*. 2013;120:334–341.
34. Bhisitkul RB, Mendes TS, Rofagha S, et al. Macular atrophy progression and 7-year vision outcomes in subjects from the ANCHOR, MARINA, and HORIZON studies: the SEVEN-UP study. *Am J Ophthalmol*. 2015;159:915–924.e2.
35. Ford KM, Saint-Geniez M, Walshe T, Zahr A, D'Amore PA. Expression and role of VEGF in the adult retinal pigment epithelium. *Invest Ophthalmol Vis Sci*. 2011;52:9478–9487.
36. Saint-Geniez M, Maharaj AS, Walshe TE, et al. Endogenous VEGF is required for visual function: evidence for a survival role on muller cells and photoreceptors. *PLoS One*. 2008;3:e3554.
37. Peters S, Heiduschka P, Julien S, et al. Ultrastructural findings in the primate eye after intravitreal injection of bevacizumab. *Am J Ophthalmol*. 2007;143:995–1002.
38. Tserentsoodol N, Gordiyenko NV, Pascual I, Lee JW, Fliesler SJ, Rodriguez IR. Intraretinal lipid transport is dependent on high density lipoprotein-like particles and class B scavenger receptors. *Mol Vis*. 2006;12:1319–1333.
39. Rudolf M, Malek G, Messinger JD, Clark ME, Wang L, Curcio CA. Sub-retinal drusenoid deposits in human retina: organization and composition. *Exp Eye Res*. 2008;87:402–408.
40. Oak AS, Messinger JD, Curcio CA. Subretinal drusenoid deposits: further characterization by lipid histochemistry. *Retina*. 2014;34:825–826.
41. Zweifel SA, Imamura Y, Spaide TC, Fujiwara T, Spaide RF. Prevalence and significance of subretinal drusenoid deposits

Investigative Ophthalmology & Visual Science

Downloaded from iovs.arvojournals.org on 12/02/2020

(reticular pseudodrusen) in age-related macular degeneration. *Ophthalmology*. 2010;117:1775–1781.

42. Steinberg JS, Auge J, Fleckenstein M, Holz FG, Schmitz-Valckenberg S. Longitudinal analysis of reticular drusen associated with age-related macular degeneration using combined confocal scanning laser ophthalmoscopy and spectral-domain optical coherence tomography imaging. *Ophthalmologica*. 2015;233:35–42.
43. Zhang Y, Wang X, Godara P, et al. Dynamism of dot subretinal drusenoid deposits in age-related macular degeneration demonstrated with adaptive optics imaging [published online ahead of print February 10, 2017]. *Retina*. doi:10.1097/IAE.0000000000001504.
44. Pumariega NM, Smith RT, Sohrab MA, Letien V, Souied EH. A prospective study of reticular macular disease. *Ophthalmology*. 2011;118:1619–1625.
45. Sarks J, Arnold J, Ho IV, Sarks S, Killingsworth M. Evolution of reticular pseudodrusen. *Br J Ophthalmol*. 2011;95:979–985.
46. Zanzottera EC, Messinger JD, Ach T, Smith RT, Freund KB, Curcio CA. The project MACULA retinal pigment epithelium grading system for histology and optical coherence tomography in age-related macular degeneration. *Invest Ophthalmol Vis Sci*. 2015;56:3253–3268.
47. Mullins RF, Schoo DP, Sohn EH, et al. The membrane attack complex in aging human choriocapillaris: relationship to macular degeneration and choroidal thinning. *Am J Pathol*. 2014;184:3142–3153.
48. Seth A, Cui J, To E, Kwee M, Matsubara J. Complement-associated deposits in the human retina. *Invest Ophthalmol Vis Sci*. 2008;49:743–750.
49. Curcio CA, Johnson M, Huang JD, Rudolf M. Apolipoprotein B-containing lipoproteins in retinal aging and age-related macular degeneration. *J Lipid Res*. 2010;51:451–467.
50. Kurihara T, Westenskow PD, Bravo S, Aguilar E, Friedlander M. Targeted deletion of VEGFA in adult mice induces vision loss. *J Clin Invest*. 2012;122:4213–4217.
51. Steinberg JS, Fleckenstein M, Holz FG, Schmitz-Valckenberg S. Foveal sparing of reticular drusen in eyes with early and intermediate age-related macular degeneration. *Invest Ophthalmol Vis Sci*. 2015;56:4267–4274.
52. Curcio CA, Sloan KR, Kalina RE, Hendrickson AE. Human photoreceptor topography. *J Comp Neurol*. 1990;292:497–523.
53. Curcio CA, Medeiros NE, Millican CL. Photoreceptor loss in age-related macular degeneration. *Invest Ophthalmol Vis Sci*. 1996;37:1236–1249.
54. Ach T, Tolstik E, Messinger JD, Zarubina AV, Heintzmann R, Curcio CA. Lipofuscin redistribution and loss accompanied by cytoskeletal stress in retinal pigment epithelium of eyes with age-related macular degeneration. *Invest Ophthalmol Vis Sci*. 2015;56:3242–3252.
55. Adler R, Curcio C, Hicks D, Price D, Wong F. Cell death in age-related macular degeneration. *Mol Vis*. 1999;5:31.
56. Sarks JP, Sarks SH, Killingsworth MC. Evolution of geographic atrophy of the retinal pigment epithelium. *Eye (Lond)*. 1988;2(Pt 5):552–577.
57. Ach T, Huisingh C, McGwin G Jr, et al. Quantitative autofluorescence and cell density maps of the human retinal pigment epithelium. *Invest Ophthalmol Vis Sci*. 2014;55:4832–4841.
58. Joachim N, Mitchell P, Rochtchina E, Tan AG, Wang JJ. Incidence and progression of reticular drusen in age-related macular degeneration: findings from an older Australian cohort. *Ophthalmology*. 2014;121:917–925.
59. Lee MY, Yoon J, Ham DI. Clinical features of reticular pseudodrusen according to the fundus distribution. *Br J Ophthalmol*. 2012;96:1222–1226.
60. Klein R, Meuer SM, Knudtson MD, Iyengar SK, Klein BE. The epidemiology of retinal reticular drusen. *Am J Ophthalmol*. 2008;145:317–326.
61. Ueda-Arakawa N, Ooto S, Nakata I, et al. Prevalence and genomic association of reticular pseudodrusen in age-related macular degeneration. *Am J Ophthalmol*. 2013;155:260–269, e262.
62. Smith RT, Sohrab MA, Busuioc M, Barile G. Reticular macular disease. *Am J Ophthalmol*. 2009;148:733–743, e732.
63. Jung JJ, Chen CY, Mrejen S, et al. The incidence of neovascular subtypes in newly diagnosed neovascular age-related macular degeneration. *Am J Ophthalmol*. 2014;158:769–779.e2.
64. Yehoshua Z, Rosenfeld PJ, Gregori G, et al. Progression of geographic atrophy in age-related macular degeneration imaged with spectral domain optical coherence tomography. *Ophthalmology*. 2011;118:679–686.
65. Forte R, Querques G, Querques L, Massamba N, Le Tien V, Souied EH. Multimodal imaging of dry age-related macular degeneration. *Acta Ophthalmol*. 2012;90:e281–e287.
66. Steinberg JS, Gobel AP, Fleckenstein M, Holz FG, Schmitz-Valckenberg S. Reticular drusen in eyes with high-risk characteristics for progression to late-stage age-related macular degeneration. *Br J Ophthalmol*. 2015;99:1289–1294.
67. Steinberg JS, Gobel AP, Fleckenstein M, Holz FG, Schmitz-Valckenberg S. Reticular drusen in eyes with high-risk characteristics for progression to late-stage age-related macular degeneration. *Br J Ophthalmol*. 2015;99:1289–1294.
68. Huisingh C, McGwin G Jr, Neely D, et al. The association between subretinal drusenoid deposits in older adults in normal macular health and incident age-related macular degeneration. *Invest Ophthalmol Vis Sci*. 2016;57:739–745.
69. Kim JH, Chang YS, Kim JW, Lee TG, Kim CG. Prevalence of subtypes of reticular pseudodrusen in newly diagnosed exudative age-related macular degeneration and polypoidal choroidal vasculopathy in Korean patients. *Retina*. 2015;35:2604–2612.
70. Xu L, Blonska AM, Pumariega NM, et al. Reticular macular disease is associated with multilobular geographic atrophy in age-related macular degeneration. *Retina*. 2013;33:1850–1862.
71. Sarks S, Cherepanoff S, Killingsworth M, Sarks J. Relationship of Basal laminar deposit and membranous debris to the clinical presentation of early age-related macular degeneration. *Invest Ophthalmol Vis Sci*. 2007;48:968–977.

Investigative Ophthalmology & Visual Science

Downloaded from iovs.arvojournals.org on 12/02/2020